Fano resonances of a curved waveguide with an embedded quantum dot

O. Olendski
Atomic and Molecular Engineering Laboratory, Belarussian State University, Skarina Avenue 4, Minsk 220050, Belarus

L. Mikhailovska
Department of Higher Mathematics, Military Academy, Minsk 220056, Belarus

(Received 16 September 2002; revised manuscript received 28 October 2002; published 15 January 2003)

A theoretical study of a waveguide with a uniformly curved section and an embedded quantum dot is presented within the envelope function approximation. For the quantum dot being extremely localized in the direction of the electron propagation, exact form of the scattering matrix of the system is derived, and a conductance of the waveguide is calculated. It is shown that if, for the straight wire with dot, in the fundamental mode conductance is a monotonically increasing function of the Fermi energy, then, after bending the waveguide, one has Fano resonances on the conductance-Fermi energy dependence. The resonances appear as a result of mixing by the bend of the longitudinal and transverse electron motion in the straight parts of the waveguide and concomitant intersubband interaction. For the small bend angle (large bend radius) the width of the resonance grows narrower with decreasing the angle (increasing the radius), until in the limit of the zero angle (infinite radius) one recovers true bound state in the continuum and the corresponding monotonic conductance of the straight channel. A dependence of the resonance width on the parameters of the bend and the dot is investigated; in particular, it is shown that, as a result of coherent resonant phenomena in the superposition of the bend and the dot, true bound states in the continuum can be formed also for the nonzero bend angle and the finite bend radius. Miscellaneous cases of bending the waveguide which, if uncurved, already exhibits the Fano resonance, are also investigated; for example, it is shown that in this situation, as a result of the bend, resonances can collapse too, again producing true bound states in the continuum. The case of inversion of the Fano resonances, i.e., a change of their minimum and maximum mutual location, is also analyzed. Mathematical and physical interpretation of the obtained results is given, and characteristic features of the critical parameters at which the Fano resonances collapse, are discussed. It is demonstrated that currents flowing in the waveguide, near the Fano resonances drastically change their behavior from laminar to vortical structure, and an evolution of the vortices is described. Parallels are drawn to the other types of the guiding structures, such as electromagnetic waveguides and acoustic ducts.

DOI: 10.1103/PhysRevB.67.035310 PACS number(s): 73.63.Nm, 03.65.Ge, 84.40.Az, 43.20.+g

I. INTRODUCTION

Fano resonance[1] is a general property of the physical systems where a degeneracy of continuum states and a discrete level raised into this continuum is present.[2] Interaction of such quasibound state with background leads to the characteristic asymmetric resonances whose line shape is described by the formula

$$f(\varepsilon)=\frac{(\varepsilon+q)^2}{\varepsilon^2+1}. \tag{1}$$

Here $\varepsilon=(E-E_R)/(\Gamma/2)$ is the dimensionless energy in units of the resonance width Γ, q is the asymmetry parameter, and E_R is the resonance energy of the Fano transition. Fano function, Eq. (1), has a minimum of zero at energy $E_{min}=E_R-\Gamma q/2$ and reaches maximum at $E_{max}=E_R+\Gamma/(2q)$. If we confine our consideration to the real values, then a positive (negative) q means that the minimum is achieved at the smaller (larger) energies than the corresponding maximum. Thus, asymmetry of the resonance is proportional to the asymmetry parameter q which, in turn, is defined by the asymmetry of the physical system itself. Fano resonances were first described in the study of the inelastic scattering spectrum of noble gases more than forty years ago[1] (though much earlier mentionings about such line shape have been made in Refs. 3–5), and they continue to attract a careful attention of the researchers from different branches of physics.[6–9]

One class of the systems where the Fano resonances are under scrutiny from transport and optical point of view, are low-dimensional semiconductor nanostructures[10–12] and, among them, quantum quasi-one-dimensional (Q1D) waveguides.[13–21] Interest in the nanometer quantum channels has been further stimulated by the experimental discovery of the conductance quantization of these man-made structures.[22,23] It was shown that a quantum dot embedded into such electron waveguide acts as an attractive scatterer and, as such, creates a quasibound state in the continuum. Mathematically this level is described by the superposition of the set of the evanescent modes localized near the dot, and one or several external plane-wave components whose amplitudes determine the escape rate, or lifetime, of the state. This quasibound state is split off from the higher-lying subband and can capture the electron. As a result, its interaction with its degenerate continuum counterpart even in the noninteracting electron model strongly affects transport properties of the waveguide creating characteristic Fano line shape on the conductance dependence on the Fermi energy. For the fundamental mode, such a Fano line develops when the quantum dot is asymmetric with respect to the middle plane

of the waveguide and, accordingly, it causes an intersubband mixing. In the opposite case of a symmetric scatterer there are no Fano resonances on conductance-Fermi energy dependence since higher-lying subbands are not involved into the transport.

On the other hand, continuous spatial reduction in the design of electronic and optical circuits inevitably introduces channels with bends connecting many separate devices on a single chip. Therefore, a correct description of the waveguides with bends becomes crucial in further development of nanotechnologies. Recently this problem was addressed widely [see reviews (Refs. 24 and 25)]. In particular, it was predicted that a bend in the otherwise uniform waveguide produces bound states spatially localized in the bent region with energies below subband thresholds.[26–32] Compared to the straight waveguide, electrons with momenta smaller than the momentum of the higher-lying subband can dwell in the extra space of the bend. The quasibound levels split off from the subbands other than the fundamental threshold, interfere destructively with their degenerate continuum counterpart leading to the steep dips in the conductance.[28,31,33–35] However, at some critical parameters of the bend these dips disappear substituted by the resonant tunneling through the bend, and a quasibound state turns into the true bound level degenerate with the continuum.[35] Bent electromagnetic waveguides were also extensively studied (see Refs. 36–38 and literature therein). Similar efforts have been undertaken for the investigation of sound propagation in rigid bends in acoustic ducts[39–43] as well. Summary of this research up to the early 1990's is given in Ref. 44. Mathematically, all these systems are described by the same type of second-order differential equation for scalar fields in two dimensions, namely, by the Helmholtz equation. The only mathematical difference between them is in the type of boundary conditions: Dirichlet, one for the electronic and transverse-electric radio waves, and Neumann condition, for the transverse-magnetic and sound waves. To emphasize the general physical significance of study of the bent waveguides, we mention that this model is used also in the investigation of quark confinement[45] in the elementary particle physics and chemical rearrangement processes and reaction rates in quantum chemistry.[46,47]

So far, influences of the bend and the quantum dot on the Q1D quantum channels were considered separately, without their interaction. In the present paper, we investigate theoretically combined influence of these two nonuniformities on the conductance of the waveguide. Within an effective mass approximation and noninteracting electron model we derive an exact expression of the scattering matrix of the curved waveguide with quantum dot embedded into the bend. The potential of the dot is extremely localized in the propagation direction and has finite dimensions in the transverse direction. Ballistic transport of the electrons is assumed throughout the paper. We show that if, for the straight waveguide with dot, conductance is a monotonic function of the Fermi energy, then for the bent structure asymmetric Fano line shape appears as a result of mixing by the bend of the transverse and longitudinal motion. For the small bend angle (large bend radius) the resonance width is getting smaller for the decreasing angle (increasing radius) until for the straight waveguide, we recover true bound state in the continuum. True bound states can also be obtained for the nonzero angles and finite bend radii, when the coherent resonant phenomena in the bend with embedded dot cancel out a possibility of the particle escape from the bend to infinity. If, on the other hand, for the straight waveguide with dot a Fano resonance already exists, applying the bend changes its characteristics leading again to the true bound states in the continuum with the corresponding substitution of the asymmetric Fano line shape by the monotonic curve. Interesting case of the inversion of the location of the conductance peak and zero is also discussed. Currents flowing in the waveguide are calculated; in particular, it is shown that a laminar flow far away from the Fano resonance turns into the vortex structure for the energies close to E_R. A comparison with a straight waveguide with impurity is performed, and a strong similarity between these two cases is pointed out. It is shown that obtained results can be applied to the similar guiding structures in other branches of physics, such as, electrodynamics and acoustics.

The paper is organized as follows. In Sec. II our model is presented and a necessary formulation is briefly given. Section III is devoted to the presentation of the calculated results and their detailed physical interpretation for various parameters of the bend and the dot. Summary of the results is provided in Sec. IV.

II. MODEL AND FORMULATION

The subject of our interest is an infinitely long Q1D waveguide of width d with a uniformly curved section of inner radius ρ_0 and angle ϕ_0 (Fig. 1). In addition, a quantum dot with the potential

$$V_{qd}(\mathbf{r}) = \frac{\hbar^2}{m^* d^2}\Omega\,\delta(\phi-\phi_{qd})\,\theta(\rho-\rho_0-S)\,\theta(L+S+\rho_0-\rho) \tag{2}$$

is embedded into the bend. The pole of the coordinate system (ρ,ϕ) coincides with the center of the bend, and the polar axis is a vertical junction between straight and bent parts of the waveguide. m^* in Eq. (2) is the effective electron mass, $\delta(x)$ is a δ function, and $\theta(x)$ is a step function. Form of the potential $V_{qd}(\rho,\phi)$ shows that we assume the quantum dot being extremely localized in the propagation direction and having the length L in the transverse direction with its lower edge shifted from the waveguide boundary by the distance S. Also, the quantum dot is shifted from the vertical junction in azimuthal direction by the angle ϕ_{qd}. Strength of the quantum dot potential is determined by the dimensionless parameter Ω. Its negative values correspond to the attractive potential (quantum dot), and the positive ones to the repulsive impurity (quantum antidot).

Within an effective-mass approximation the time-independent Schrödinger equation for noninteracting electrons describes the particle wavefunction $\Psi(\mathbf{r})$,

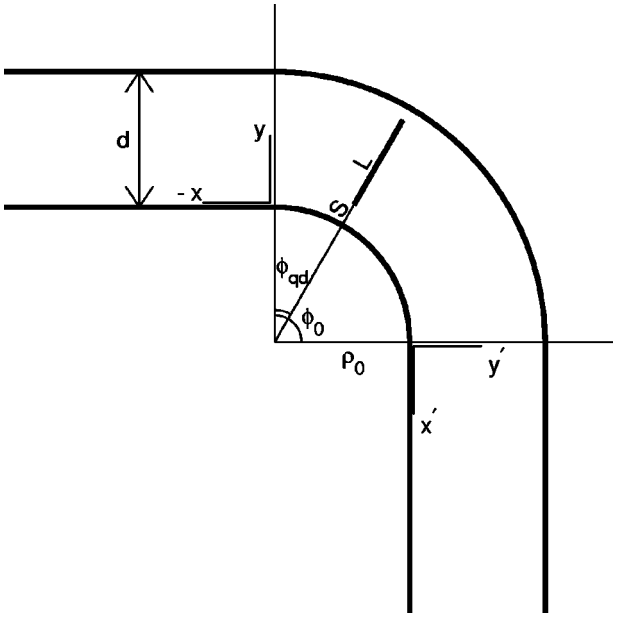

FIG. 1. Schematic picture of the bent quantum waveguide of constant width d with short-range impurity of the length L inside the bend. Bend inner radius and angle are ρ_0 and ϕ_0, respectively. Impurity is shifted from the upper junction in azimuthal direction by the angle ϕ_{qd} and from the lower wall by the distance S. Impurity strength is $\hbar^2/(m^*d^2)\Omega$. Local rectangular coordinate systems (x,y) and (x',y') for the straight arms are also shown.

$$-\frac{\hbar^2}{2m^*}\vec{\nabla}^2\Psi(\mathbf{r})+V(\mathbf{r})\Psi(\mathbf{r})=E\Psi(\mathbf{r}) \tag{3}$$

with the potential $V(\mathbf{r})$ containing contributions from the waveguide V_{wq} and the dot V_{qd},

$$V(\mathbf{r})=V_{wg}(\mathbf{r})+V_{qd}(\mathbf{r}). \tag{4}$$

For the hard-wall boundary conditions we accept in this paper, $V_{wg}(\mathbf{r})$ is zero inside the waveguide and infinity otherwise.

Transport properties of the waveguide are determined by the scattering matrix $\mathbf{S}(E)$. For finding it, we proceed in the same way as in the case of a dot-free curved waveguide;[35] namely, in each of the region we expand solution of Eq. (3) in a set of known analytical functions and match them at the boundaries. In particular, inside the bend we have the following solutions:

$$\Psi(\rho,\phi)=\sum_{n=1}^{\infty} R_n(\rho)[D_n^{(1)}\sin(\nu_n\phi) + F_n^{(1)}\cos(\nu_n\phi)], \quad 0\leqslant\phi\leqslant\phi_{qd}, \tag{5}$$

$$\Psi(\rho,\phi)=\sum_{n=1}^{\infty} R_n(\rho)\{D_n^{(2)}\sin[\nu_n(\phi-\phi_{qd})] + F_n^{(2)}\cos[\nu_n(\phi-\phi_{qd})]\}, \quad \phi_{qd}\leqslant\phi\leqslant\phi_0, \tag{6}$$

with $R_n(\rho)$ being a radial part of the wave function:

$$R_n(\rho)=Y_{\nu_n}\left[\left(\frac{2m^*E}{\hbar^2}\right)^{1/2}\rho_0\right]J_{\nu_n}\left[\left(\frac{2m^*E}{\hbar^2}\right)^{1/2}\rho\right] - J_{\nu_n}\left[\left(\frac{2m^*E}{\hbar^2}\right)^{1/2}\rho_0\right]Y_{\nu_n}\left[\left(\frac{2m^*E}{\hbar^2}\right)^{1/2}\rho\right]. \tag{7}$$

Here $J_\nu(x)$ and $Y_\nu(x)$ are Bessel functions of the first and second kind, respectively.[48] Detailed analysis of the functions (7) and the coefficients ν_n is given in Ref. 35. Coefficients $D_n^{(i)}$ and $F_n^{(i)}$, $i=1,2$, $n=1,2$, etc. are to be found from matching wave functions in the different regions. Matching wave function for the azimuthal δ potential, Eq. (2), is done similar to the one-dimensional rectangular case[49] or to the potential having a peculiarity in the radial direction:[50]

$$\Psi(\rho,\phi_{qd}-0)=\Psi(\rho,\phi_{qd}+0), \tag{8a}$$

$$\frac{1}{\rho}\frac{\partial}{\partial\phi}\Psi(\rho,\phi)\bigg|_{\phi=\phi_{qd}+0}-\frac{1}{\rho}\frac{\partial}{\partial\phi}\Psi(\rho,\phi)\bigg|_{\phi=\phi_{qd}-0} = \frac{2}{d}\Omega\,\theta(\rho-\rho_0-S)\,\theta(L+S+\rho_0-\rho)\Psi(\rho,\phi_{qd}). \tag{8b}$$

Quite naturally, Eq. (8a) shows that the wave function remains continuous at the δ peculiarity, and Eq. (8b) manifests that a jump of its azimuthal derivative $(1/\rho)\partial\Psi/\partial\phi$ is proportional to the strength of the potential discontinuity Ω.

From the obtained system of equations it is possible to derive an expression linking amplitudes of transmitted and incoming modes, i.e., to define a scattering matrix $\mathbf{S}(E)$ which is a function of the electron energy E. It also depends on the parameters ρ_0, ϕ_0, ϕ_{qd}, Ω, L, S. We do not write its explicit form here, mentioning only that in the limiting cases 1) $\Omega=0$, $\phi_{qd}=0$ or 2) $L=0$ it turns, as would expected, into the expression for the dot-free curved waveguide.[35] Its knowledge allows one to calculate the two-probe total conductance G,[51]

$$G(E)=\frac{2e^2}{h}\sum_{nn'}\frac{k_{n'}}{k_n}S^*_{nn'}S_{nn'}, \tag{9}$$

where k_n is the electron wave vector of the channel n and the scattering matrix element $S_{nn'}$ defines the probability of the electron scattering from channel n to n'. The sum in Eq. (9) runs over all open channels, and E is a Fermi energy, i.e., an energy of the highest occupied level. For the single propagating mode this equation reduces to

$$G(E)=\frac{2e^2}{h}|S_{11}|^2. \tag{10}$$

The following section is devoted to the analysis of Eq. (10) for various parameters of the dot and the bend.

III. RESULTS AND DISCUSSION

We will consider below transport properties in the fundamental mode only: $\pi^2\hbar^2/(2m^*d^2)\leqslant E\leqslant 4\pi^2\hbar^2/(2m^*d^2)$,

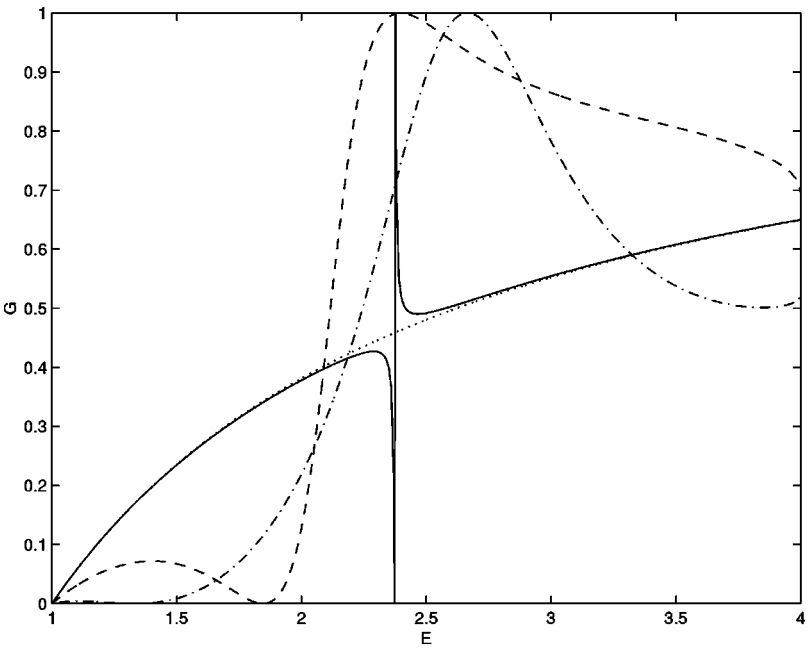

FIG. 2. Conductance G as a function of the Fermi energy E for $\rho_0=0.01$, $L=1$, $\Omega=-4$, $\phi_{qd}=\phi_0/2$ and several values of ϕ_0: the dotted line is for $\phi_0=0$ (straight waveguide), the solid line is for $\phi_0=5°$, the dashed line is for $\phi_0=90°$, and the dash-dotted line is for $\phi_0=180°$.

thus excluding an interference between different propagating modes. From the two-band approximation it is known that in this case for the straight waveguide a Fano line develops on the conductance-Fermi energy dependence when the intersubband matrix element is not zero.[17,19,21] It can be shown that for any longitudinally symmetric potential $V_{qd}(\mathbf{r})$ from Eq. (4) the conductance G [in units of $(2e^2/h)$] is expressed as[18]

$$G=\frac{1}{1+q^2}\,\frac{(E-E_R+q\Gamma)^2}{(E-E_R)^2+\Gamma^2}. \tag{11}$$

In terms of Eq. (1) we can say that in our case $\varepsilon=(E-E_R)/\Gamma$. Equation (11) shows that the conductance not only reaches minimum of zero at $E_{min}=E_R-\Gamma q$, but also the maximum value that is achieved at $E_{max}=E_R+\Gamma/q$, is an exact unity. So, for our δ potential the scattering matrix element S_{11} defining the conductance, near the Fano transition of the straight waveguide takes the form[19,20]

$$S_{11}(E)=\frac{1}{(1+q^2)^{1/2}}\,\frac{E-E_{min}}{E-E_{max}+\Gamma/q+i\Gamma}, \tag{12}$$

where E_{min} is the energy of the minimum conductance of zero, E_{max} is the energy where the maximum transmission of unity is achieved, $E_R=(E_{max}+E_{min})/2+(q-1/q)\Gamma/2$, $E_{max}-E_{min}=(q+1/q)\Gamma$. The resonance width Γ is proportional to the square of the nondiagonal element of the intersubband transition matrix, and the asymmetry parameter q depends only on the background (nonresonant) transmission. In the opposite case of the absence of intersubband interaction the conductance is a monotonically increasing function of the Fermi energy,[16,17,21] and a bound state is raised into the continuum.[15–17] It is a true bound state with infinite lifetime, since due to the different transverse parity it does not interact with its degenerate continuum counterpart.[16,17] For our model potential which for the straight channel takes the form

$$V_{qd}(\mathbf{r})=\frac{\hbar^2}{m^*d}\,\Omega\,\delta(x)\,\theta(y-S)\,\theta(L+S-y), \tag{13}$$

intersubband scattering is zero when the potential is symmetric with respect to the middle plane of the waveguide: $S=(1-L)/2$. Since for the straight channel situations with symmetrically and asymmetrically embedded dot differ qualitatively, below for the bent waveguide we consider them separately. We will measure all distances in units of the waveguide width d, all energies—in units of $\pi^2\hbar^2/(2m^*d^2)$, conductance—in units of $(2e^2/h)$, and time—in units of $2m^*d^2/(\pi^2\hbar)$. Also, we do not consider the physically irrelevant angles larger than 180°.

A. Transversely symmetric quantum dot: $S=(1-L)/2$

For the bent waveguide, apart from the transverse symmetry of the embedded quantum dot, another symmetry comes into the play; namely, for the clean waveguide the system is symmetric with respect to reflection about the line $\phi=\phi_0/2$. Therefore, cases of $\phi_{qd}=\phi_0/2$ and $\phi_{qd}\neq\phi_0/2$ also will be considered separately.

Let us start from the situation with $\phi_{qd}=\phi_0/2$. As it was just mentioned, for the straight waveguide we have a true bound state which does not interact with the continuum, since they are effectively decoupled by the parity conservation. The wave function of this level localized near the dot contains in the straight arms only fading exponents, without plane-wave component. Imposing a bend, one mixes longitudinal and transverse motions in the straight arms and, accordingly, adds freely propagating trigonometric constituent to the wave function. As a result, intersubband interaction ceases to be zero, and Fano resonances appear in the transmission spectrum. Figure 2 shows the conductance G as a function of the Fermi energy E for $\Omega=-4$, $\rho_0=0.01$, and several values of ϕ_0. The dot is tightly embedded into the waveguide with its length being equal to the waveguide

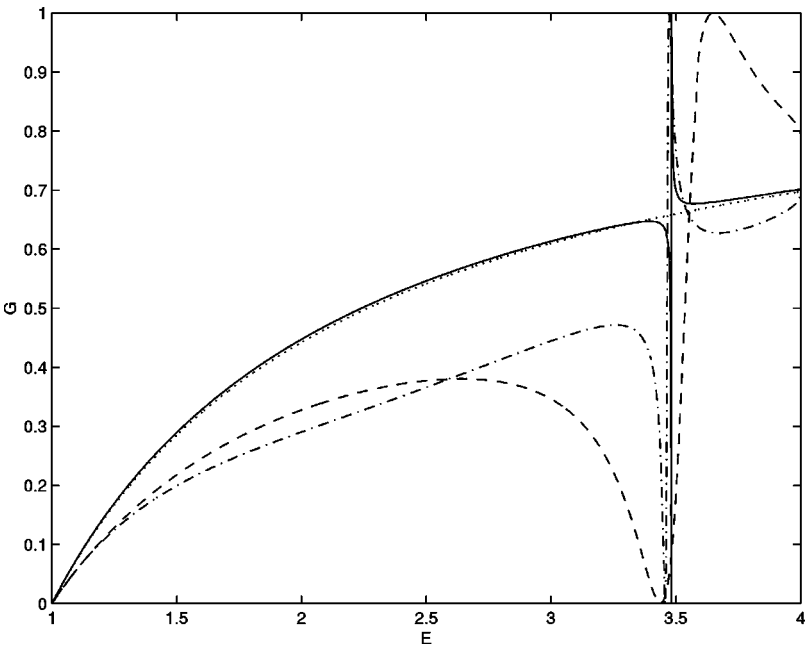

FIG. 3. The same as in Fig. 2 for $L=0.5$ and $S=0.25$ with all other mentioned in Fig. 2 parameters being unchanged.

width, $L=1$. We see that a monotonic curve for the straight waveguide transforms into the asymmetric Fano resonance as soon as the bend is introduced. The closer ϕ_0 to zero, the sharper the resonance is. Quantitatively, it can be described by the value of Γ which is a monotonically increasing function of the bend angle ϕ_0. This means that the square of the intersubband matrix element increases with the bend angle growing. The same behavior of the conductance was theoretically observed for the small magnetic field imposed onto the quantum channel with the embedded dot.[16] In both cases an imposed perturbation—either bend or magnetic field—destroys the transverse symmetry of the system, thus coupling the bound state with the continuum, transforming the former into the quasibound level, and leading to the characteristic Fano resonances with their widths—at least, for the small and moderate disturbances—proportional to the strength of the perturbation. For all values of the bend angle and radius, maximum conductance is equal to unity, and the minimum transmission is exactly zero.

In understanding properties of the bent waveguides with impurities, it is convenient to use approximation that maps processes in the impurity-free bend onto the motion in the straight waveguide with the potential which creates the wave function[28]

$$\Psi_n(\rho,x)=\frac{1}{\sqrt{\rho}}\sin[n\pi(\rho-\rho_0)]\Phi_n(x) \tag{14}$$

with the longitudinal variable $x=(\rho_0+1/2)\phi$ (see also Ref. 30). Function $\Phi_n(x)$ describes the motion in a one-dimensional square-well potential of depth $(2\pi)^{-2}(\rho_0+1/2)^{-2}$ and width $(\rho_0+1/2)\phi_0$:

$$\frac{\partial^2\Phi_n}{\partial x^2}+\left[\pi^2(E-n^2)+\frac{1}{4(\rho_0+1/2)^2}\right]\Phi_n=0,$$

$$0\leqslant x\leqslant(\rho_0+1/2)\,\phi_0\,. \tag{15}$$

The approximation, Eqs. (14) and (15), is getting better for the larger bend radius ρ_0. If we treat the square root of ρ in Eq. (14) as constant, as it was done in Ref. 28, then different channels decouple, and we have one or several true bound states in the continuum, as it was discussed in Ref. 16. However, if we lift the demand of constant square root, as it actually should be, intersubband matrix elements of the set of the functions (14) are not zeros, and various channels interact with each other. Accordingly, after inserting into the bend a δ potential with a true bound state, one can expect this state transforming into the quasibound level accompanied by the Fano structure in the transmission. In other words, effective potential of the bend causes intersubband interaction leading to the asymmetric Fano resonances.

To shed more light on this phenomenon, we show in Fig. 3 the conductance for $L=0.5$ (and, accordingly, $S=0.25$) with all other parameters being the same as in Fig. 2. Since now $L<1$, the quantum dot binds the electron weaker compared to the previous case. As a result, upon bending the waveguide one can expect formation of the Fano resonances closer to the first excited subband threshold. This is exactly that is seen in Fig. 3, where the Fano resonances are shifted upwards on the energy axis compared to Fig. 2. Another feature of Fig. 3 is the fact that the resonance width Γ is not a monotonically increasing function of the bend angle. In Fig. 4 we plot the value of $\Delta=E_{max}-E_{min}$ as a function of ϕ_0 for several values of the quantum dot lengths L. As we noted above, a value of Δ is proportional to the resonance width, $\Gamma=q\Delta/(1+q^2)$. Thus, the negative values of Δ correspond to the negative asymmetry parameter q in Eq. (1). We observe that for the small and moderate values of L (for example, $L=0.2$ in Fig. 4) the magnitude of Δ increases, reaches maximum, then decreases, reaches zero, for some angle interval becomes negative, achieves negative minimum, after which it crosses zero for the second time, and later it grows again. Since modulus of the negative values of Δ and the angle interval they occupy, are quite small, they

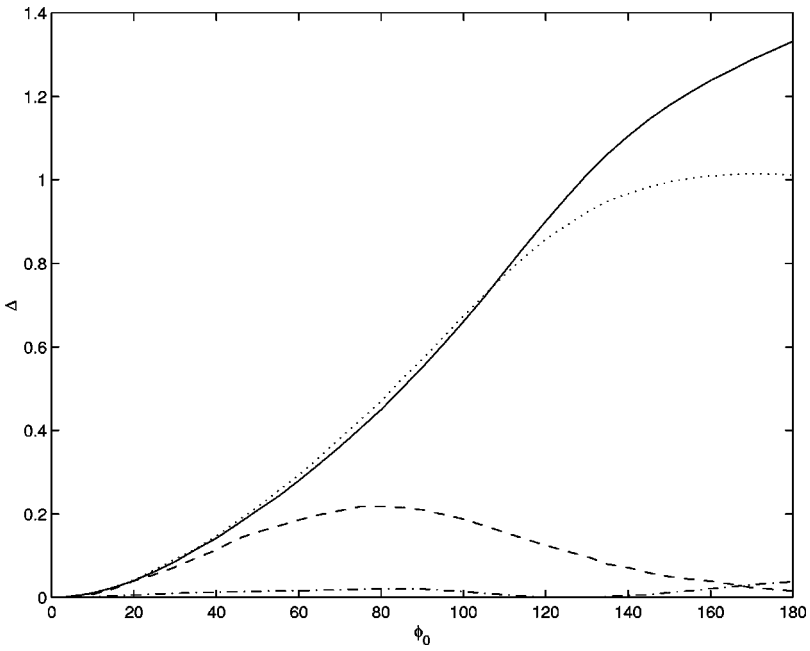

FIG. 4. Value of $\Delta = E_{max} - E_{min}$ as a function of the bend angle ϕ_0 for $\rho_0 = 0.01$, $\phi_{qd} = \phi_0/2$ and several values of the length L: the solid line is for $L = 1$ ($S = 0$), the dotted line is for $L = 0.8$ ($S = 0.1$), the dashed curve is for $L = 0.5$ ($S = 0.25$), and the dash-dotted curve is for $L = 0.2$ ($S = 0.4$).

are not resolved in Fig. 4. Also, since this feature is characteristic for the asymmetrically embedded dot as well, we defer its detailed discussion to Sec. III B, concentrating here instead on the case of the resonance width being absent. A zero value of Γ means that at these critical parameters of the system we have again a true bound state—a state with infinite lifetime. As a result of the resonant interference in the bend with embedded scatterer, a plane-wave component of the quasibound state vanishes, transforming it into the true bound state in the continuum. Similar to the case of the straight channel or the defect-free bent waveguide, this true bound state does not interact with the continuum, since they are again effectively decoupled. True bound states degenerate with the continuum, appear as very special solutions of the Schrödinger equation. They were discussed for the first time soon after the formulation of the quantum mechanics,[52] and were later extensively studied in various physical systems.[16,20,21,24,35,53,54] The conductance at the critical parameters is, as in the case of $\phi_0 = 0$, a monotonic function of the Fermi energy. We can also qualitatively explain the earlier approach by Γ to zero on the ϕ_0 axis for the smaller dot lengths L. Namely, for the smaller L, as we mentioned, the bound state energy E_{bs} is closer to the upper threshold of $E = 4$. Accordingly, the longitudinal de Broglie wavelength $\lambda_{bs} = 2/(E_{bs}^{1/2} - 1)$ of the bound state is smaller. On the other hand, for the fixed Ω a resonant condition of the bound state is determined, in the first approximation, by the length of the arc $(\rho_0 + 1/2)\phi_0$. Therefore, for the smaller dot lengths L a first resonant condition when only one half of the wavelength λ_{bs} is accommodated by the bend with dot, is achieved for the smaller angles. As is seen from Fig. 4, for $L \geqslant 0.5$ (and $\Omega = -4$) this resonant condition is achieved beyond the range of $0 \leqslant \phi_0 \leqslant 180°$; however, for the other parameters of the bend and the dot one can observe several bound states at $\phi_0 \leqslant 180°$. This explanation is similar to the description of the different number of the bound states for different radii for the clean bend.[35]

Figure 5 shows the conductance G for several bend radii ρ_0 with quantum dot tightly embedded into the waveguide and the right bend angle $\phi_0 = 90°$. It shows many similarities with Fig. 2. In particular, we see that a Fano line shape that is sharp for the large bend radius, acquires bigger width Γ with decreasing ρ_0. The larger bend radius, similar to the smaller bend angle, presents a lesser perturbation to the electron motion in the straight waveguide; accordingly, it causes a smaller intersubband interaction with its amplitude being proportional to the width of the asymmetric resonance. And in the limit of $\rho_0 \to \infty$, as it was for $\phi_0 = 0$, asymmetric Fano line shape becomes the monotonic curve of the straight waveguide with the corresponding true bound state in the continuum. For the small radius there is a considerable intersubband interaction, and so, the Fano resonances grow broader. For the very small radii the further decrease of ρ_0 cannot change noticeably the line shape; for example, there is only a slight difference between the curves for $\rho_0 = 0.01$ and $\rho_0 = 0.001$. Qualitatively, it again can be understood from Eqs. (14) and (15), where for the very small ρ_0 its variation has a marginal effect on their solutions. Thus, we see that, contrary to the case of the small magnetic field applied to the straight waveguide[16] when only one parameter—magnetic-field intensity—controls the sharpness of the resonances, one has both the bend radius and the bend angle for varying the line shape of the Fano profiles in the curved waveguide.

The coupling of the longitudinal and transverse motion near the Fano transition in the bend with impurity can be vividly demonstrated when one considers the currents flowing in the waveguide. It follows from the familiar quantum mechanical expression for the current[55] density $\vec{j}$ that it is proportional to $\mathrm{Im}(\Psi \vec{\nabla} \Psi^*)$. As a representative example, we take a configuration with $\rho_0 = 0.01$, $\phi_0 = 5°$, and $L = 1$ (solid curve in Fig. 2). In Fig. 6 current-density patterns are shown for several Fermi energies. If the energy is far away

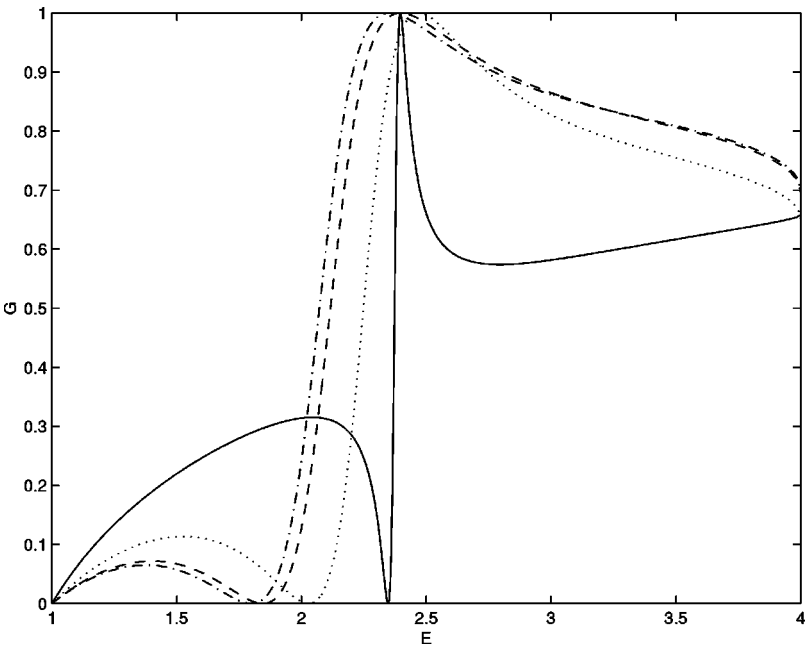

FIG. 5. Conductance G as a function of the Fermi energy E for $L=1$, $\Omega=-4$, $\phi_0=90°$, $\phi_{qd}=\phi_0/2$ and several values of ρ_0: the solid line is for $\rho_0=1$, the dotted line is for $\rho_0=0.1$, the dashed line is for $\rho_0=0.01$, and the dash-dotted line is for $\rho_0=0.001$. The resonance gets broader as the bend radius ρ_0 decreases.

from the resonance, the flow of the electrons is perfectly laminar. When E approaches E_{min}, a vortex starts to build up in the bend region. One of the initial stages of the formation of such a vortex is shown in Fig. 6(a) which corresponds to the first maximum in Fig. 2 with $G=0.427$. It is seen that far away from the bend the current has a longitudinal component only; however, in the bend region and its immediate neighborhood a transverse part which was negligible in the straight arms, is clearly visible. For the energy in Fig. 6(a) a formation of the vortex is not complete, but the current density quickly acquires a circular form with further decrease of G, and after $E\sim 2.33$ we have a closed vortex. Similar vortices of the currents were found before in the straight nonuniform[16,56,57] and bent clean waveguides.[58] For the quantum channel we consider in this paper, a remarkable feature of such a vortical flow is an abrupt change of the direction of its rotation after passing the minimum of the Fano resonance. For example, Fig. 6(b) shows the currents for the energy immediately left from the Fano minimum with $G=3.167\times 10^{-7}$ and a clockwise rotation. At the minimum the direction of the rotation abruptly changes to the counterclockwise one and retains it for the higher energies, as it is seen in Fig. 6(c), which corresponds to the conductance $G=0.633$ and energy between the Fano extrema. An analogous abrupt reversal of the current after passing a minimum of the conductance takes place for the bent defect-free quantum channel.[58] The vortex structure starts to resolve for the Fermi energies to the right of the Fano maximum; for example, Fig. 6(d) shows this process for $G=0.505$. Thus, similar to the clean bent waveguide,[58] minute changes in the Fermi energy may produce drastic changes in the flow of the electrons. Amplitude of the currents in the vortex is a few orders of magnitude larger than the flow far away from the bend. For the zero transmission we can interpret the vortex structure as a situation when the electron entering the waveguide from the left, reaches the bend, starts to move along a circular orbit, and after time $\tau\sim 1/\Gamma$ is reflected back. As a result, the current is totally subdued. In the same way, when the conductance has a maximum, the electron circularly rotates in the bend, and after completing a number of loops determined by E, ρ_0, ϕ_0, Ω, it leaves the curved section and propagates further into the second straight arm, thus producing a complete transmission. Of course, such a semiclassical description has a very limited scope, since the quantum effects described here do not have a classical analog.

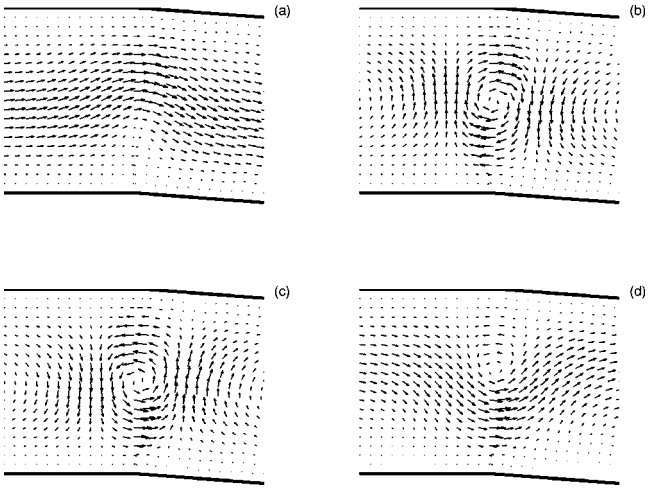

FIG. 6. Spatial distribution of the current density $\vec{j}$ for $\rho_0=0.01$, $\phi_0=5°$, $L=1$ and several values of the Fermi energy: (a) $E=2.29$, (b) $E=2.37335$, (c) $E=2.375$, and (d) $E=2.41$. Larger arrows denote higher currents. For each of the figures its own arbitrary units of the current density are used.

Let us turn now to the case of $\phi_{qd}\neq\phi_0/2$. Imposing a bend with $\phi_{qd}=\phi_0/2$ destroys the transverse symmetry of the waveguide; however, some kind of symmetry which we can call a longitudinal one, still persists; namely, waveguide remains unchanged after reflection with respect to the plane

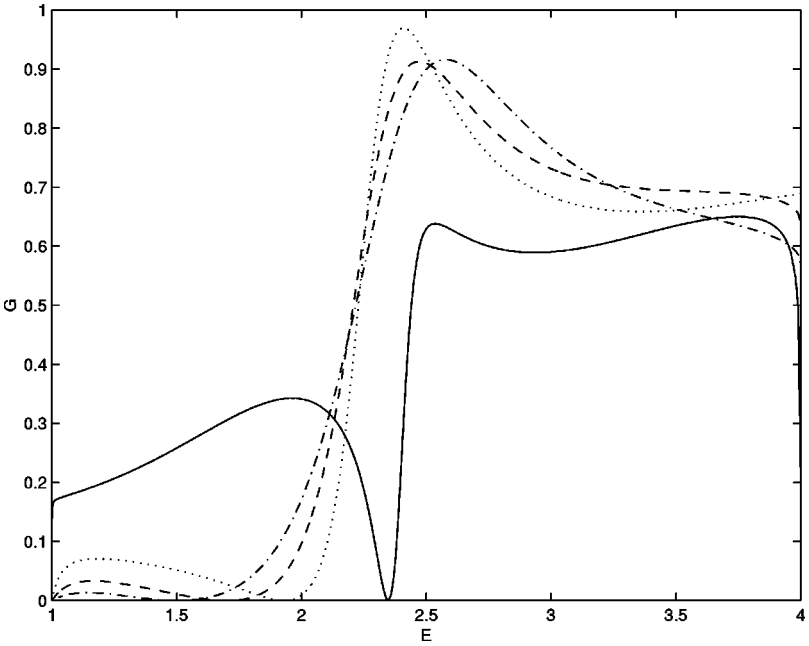

FIG. 7. Conductance G versus the Fermi energy E for $L=1$, $\Omega=-4$, $\rho_0=0.01$, $\phi_0=180°$ and several values of ϕ_{qd}: the solid line is for $\phi_{qd}=0°$, the dotted line is for $\phi_{qd}=30°$, the dashed line is for $\phi_{qd}=45°$, and the dash-dotted line is for $\phi_{qd}=60°$. For each of the curve minimum conductance is zero.

$\phi=\phi_0/2$. By shifting the dot from the middle line of the bend, this longitudinal symmetry is broken. Recalling the approximation of Eqs. (14) and (15), we can say that the dot and the bend in this case present an effective potential that is not symmetric in the direction of the wave propagation in the continuously straight channel. A case of similar asymmetric dot embedded into the straight waveguide was studied very recently.[21] Our results shown in Fig. 7 for the bent waveguide, in a sense, are similar to those in Ref. 21 for the straight channel. We see in this figure a series of Fano resonances with their minimum transmission still being zero, i.e., we observe again a complete interference blockade of the electron transport. However, maximum conductance of the system is smaller than unity and varies with ϕ_{qd}. Such decrease may be explained by the partial destruction of the coherence in the asymmetric potential.

B. Transversely asymmetric quantum dot: $S\neq(1-L)/2$

Contrary to the case $S=(1-L)/2$, now for the straight waveguide we have the Fano resonance on the conductance-energy dependence. For $S<(1-L)/2$ [$S>(1-L)/2$] the dot is shifted downward [upward] from the middle plane of the waveguide, and conductance is the same for the two shifts, S and $1-L-S$. Applying the bend to the structure modifies Fano line shape, but minimum and maximum transmission magnitudes preserve, for the case of $\phi_{qd}=\phi_0/2$, their values of zero and unity, respectively. The above mentioned degeneracy of the conductance now is lifted, the up-turn and down-turn bends are not equivalent, as they were in Sec. III A. Similar nonequivalence takes place for the defect-free bent waveguide in the uniform magnetic field[34] where, from the symmetry properties, the change of the bend from one direction to the other has the same effect as an inversion of the magnetic field. In the same way, in our case a bend in one direction with the shift S is nothing else as a bend in the opposite direction with the shift $1-L-S$.

Figure 8 shows the value of Δ as a function of the bend angle ϕ_0 for the up- and down-turn bends and radii $\rho_0=0.01$ and 0.1 with $S=0.1$, $L=0.5$, $\Omega=-4$, and $\phi_{qd}=\phi_0/2$. For the straight waveguide at these parameters we have a Fano resonance with $\Delta=0.207$. It is seen that if the bend is in (opposite to) the direction of the dot shift, then the resonance width decreases (increases) for the small and moderate angles ϕ_0. This can be accounted for as follows. The magnitude of the resonance width is a quantitative expression of the broadening of the discrete state due to its coupling to the continuum which, in turn, is determined by the asymmetry of the system. For our model an asymmetry of the waveguide is determined by the distribution of the potential with respect to the most symmetric point of the waveguide; i.e., for the straight waveguide—by the location of the dot with respect to the potential-free part and with respect to the point $x=0$, $y=1/2$. We can say that for a nonzero Γ a center-of-the-mass of the distribution of the potential is shifted from the middle of the waveguide. When the waveguide is bent, one needs to find a distribution of the potential with respect to the point $\rho=\rho_0+1/2$, $\phi=\phi_0/2$. The down-turn bend lowers locations of the potential-free straight arms relatively to this point, as it can be seen from Fig. 1. Accordingly, if the dot in the straight waveguide was shifted downward, the bend moves it upward with respect to the potential-free regions; center-of-the-mass of the distribution of the potential comes closer to the center of the waveguide; total effective potential becomes more symmetric, thus lowering Γ. Of course, such a simplified qualitative reasoning cannot describe the whole spectrum of the phenomena in the system, when a direct numerical evaluation is needed.

Now, we turn to the above mentioned inversion of the Fano resonances. As a representative example, we take the case of $\rho_0=0.01$ and down-turn bend. Figure 9 shows a part of the solid line of Fig. 8 in the range where it is close to the critical parameters. We observe that decreasing Δ turns to

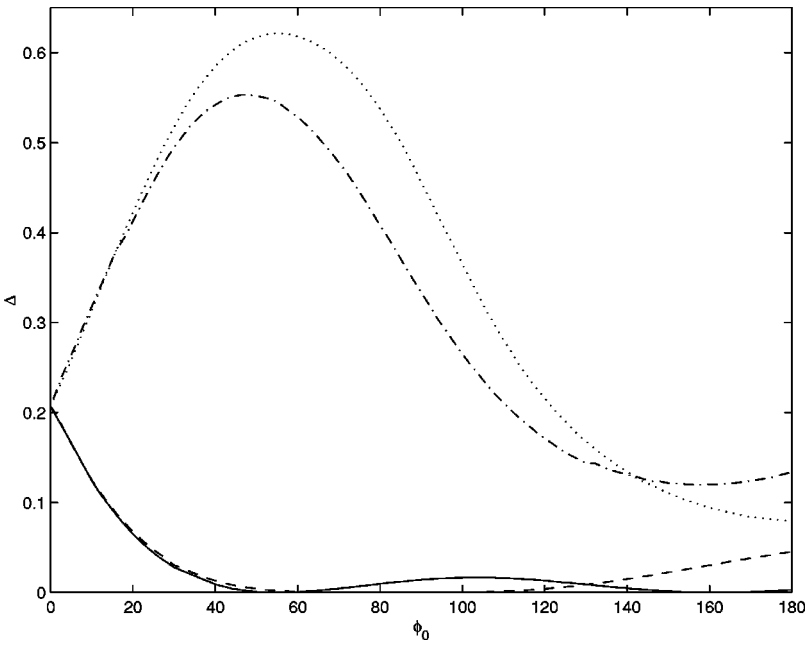

FIG. 8. Difference Δ as a function of the bend angle ϕ_0 for $L=0.5$, $S=0.1$, $\Omega=-4$, $\phi_{qd}=\phi_0/2$ and several values of the bend radius ρ_0 and different directions of the bend: the solid line is for $\rho_0=0.01$ and down-turn bend, the dotted line is for $\rho_0=0.01$ and up-turn bend, the dashed line is for $\rho_0=0.1$ and down-turn bend, and the dash-dotted line is for $\rho_0=0.1$ and up-turn bend.

zero at $\phi_0=55.040\,458°$ (thus, we have here a true bound state in the continuum which was discussed earlier), becomes negative, at $\phi_0\simeq 55.12°$ reaches minimum of $\Delta\simeq -1.67\times 10^{-7}$, after which it crosses zero again at $\phi_0=55.195\,065°$—producing the second bound state in the continuum, and grows positive. Negative value of Δ means that the maximum of the Fano resonance on the conductance-Fermi energy dependence is achieved earlier than the corresponding minimum. This is shown in Fig. 10 where the conductance for the opposite signs of Δ is shown as a function of the Fermi energy. It is seen that for positive Δ a minimum of the conductance is achieved on the energy axis before the corresponding maximum, while for the negative Δ a situation is reversed, minimum conductance of zero follows after the maximum of unity. As we have stated before, such a situation corresponds to the negative asymmetry parameter q in Eq. (1). Similar collapse and inversion of the Fano resonance in the straight waveguide was calculated earlier while changing the impurity parameters.[20,21] In particular, in Ref. 21 a collapse of the Fano resonances and a corresponding formation of the even (odd) bound state in the continuum with the variation of the longitudinal dimension of the finite-range dot was explained as a result of the intersection of the symmetric (antisymmetric) levels of two quantum wells with depths V_{22} and $E_2-E_1+V_{11}$, where V_{ii} $(i=1,2)$ are diagonal matrix elements of the impurity potential, and E_1, E_2 are the thresholds for the fundamental and the first excited subband, respectively. Accordingly, range of the longitudinal lengths of the dot between alternating even and following after it odd bound state corresponds to the

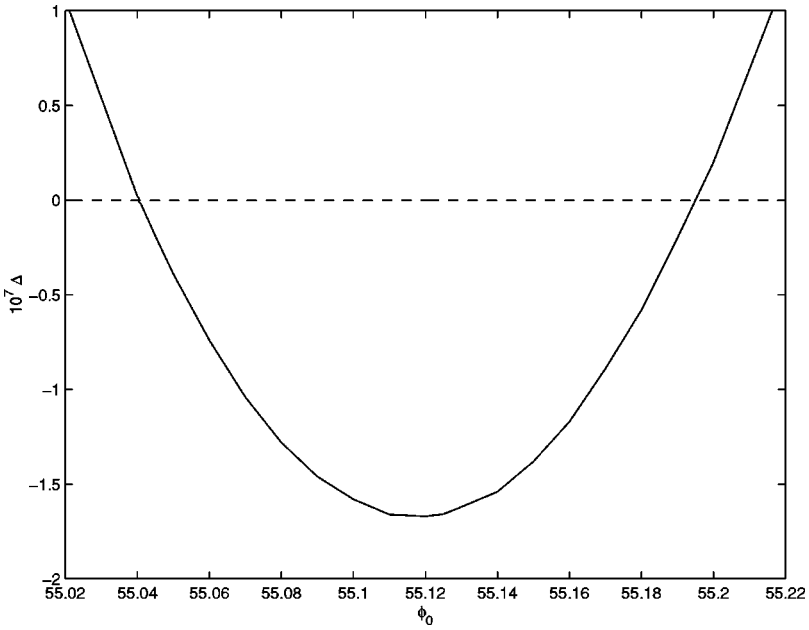

FIG. 9. Enlarged view of the solid curve of Fig. 8 near the critical values of the angle ϕ_0. Dashed line denotes zero value of the resonance width.

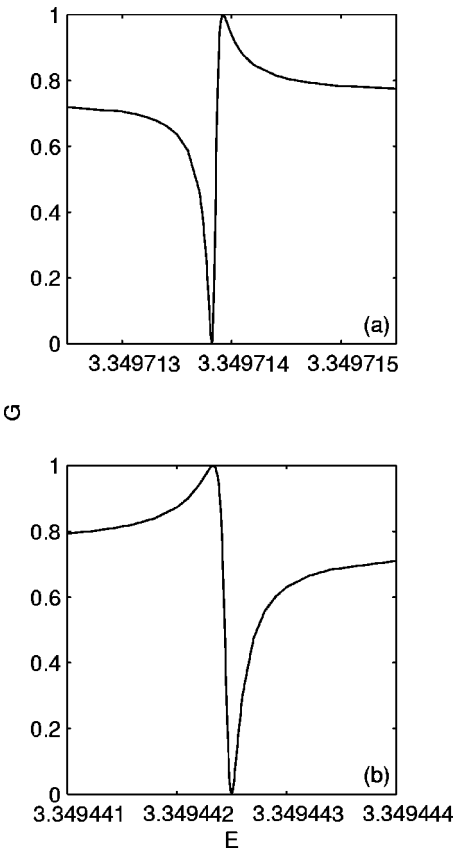

FIG. 10. Conductance G as a function of the Fermi energy for $\rho_0=0.01$ with all other parameters from Fig. 8 for two angles: (a) $\phi_0=55.02°$ (positive Δ) and (b) $\phi_0=55.12°$ (negative Δ). Due to the sharpness of the resonances different ranges of energies were used for the cases (a) and (b).

inversed Fano resonances, as the interaction between the subbands changes its sign. In the same way, for the structure we study, Fig. 9 shows a symmetric bound state at $\phi_0=55.040\,458°$, and antisymmetric bound level at $\phi_0=55.195\,065°$. As we see, for the chosen parameters these two states are located very close to each other on the ϕ_0 axis and are almost degenerate in energy. Similar situation of almost degenerate even and odd states is well known for the one-dimensional case, for example, for the interaction of the δ-potential with rectangular[49,59] or parabolic[59,60] well. Using this similarity, we see that the dot influence is much larger, and the bend mainly plays a role of the Fabry-Perot resonator[61] with junctions of the bend with the straight arms corresponding to the mirrors of the electronic resonator. Analogous approach to the degeneracy between symmetric and antisymmetric bound states in the continuum was calculated for two parallel short-range potentials in the straight quantum channel on the increase of the distance between these impurities[19] and for the scissor-shaped waveguide with the angle between the arms going to zero.[54] Varying parameters of the bend and embedded dot changes distance between the even and odd states and minimum value of Δ. For example, for the smaller bend radius the separation between symmetric and antisymmetric bound states increases with the absolute value of the minimum $|\Delta_{min}|$ increasing as well. In turn, growing radius ρ_0 which in the model of Eqs. (14) and (15) corresponds to the shallower and wider well, leads to the shrinkage of the range of the angles where the inversed Fano resonances can be observed, and for the large enough ρ_0 bound states disappear. Figure 8 shows that, depending on the bend radius, such alternating sequences of the even and odd bound states may be repeated a few times for $0°\leqslant\phi_0\leqslant180°$. Also, we remind again that such inversion takes place for both transversely symmetric as well as asymmetric dot. Therefore, all discussion of this paragraph is directly applicable to the corresponding part of Sec. III A.

A substantial increase of the negative values of Δ and the range of the angles where the inversion of the Fano resonances takes place, is achieved for the angles $\phi_{qd}\neq\phi_0/2$. In Fig. 11 the conductance G is shown for $\phi_0=180°$ and several values of ϕ_{qd}. It is seen that depending on the quantum dot angle, the conductance exhibits either positive or negative Δ on its Fano line shape. However, contrary to the case $\phi_{qd}=\phi_0/2$, the remarkable feature here is the absence of the bound states for the azimuthally asymmetric dot. Accordingly, formation of the curve with the negative difference Δ is also different. Namely, as it is seen from Fig. 11, for $\phi_{qd}=\phi_0/2$ we have a Fano resonance with positive $E_{max}-E_{min}$ and minimum conductance of zero and maximum of unity, as we discussed before. Shifting the dot from the plane $\phi_{qd}=\phi_0/2$ has two consequences: first, the pole of the resonance becomes smaller than unity and broadens, and, second, the maximum which precedes the Fano minimum on the energy axis, narrows and increases, simultaneously moving towards the minimum. We note that, similar to Sec. III A, minimum conductance is always zero, and its maximum is lower than unity for $\phi_{qd}\neq\phi_0/2$. On further dot movement away from the plane of the symmetry both maxima get the equal magnitude at some ϕ_{qd} (for example, for the parameters in Fig. 11 it takes place at $\phi_{qd}\simeq74°$) still separated by the zero minimum, which means that we do not have a true bound state here. For the smaller ϕ_{qd} the pole of the Fano resonance should be associated with the left peak, since it exceeds the magnitude of the right broad maximum. This means that the location of the extrema of the resonance is switched from ''zero-pole'' to ''pole-zero'' location. Thus, for this configuration of the system the difference $E_{max}-E_{min}$ abruptly changes it sign without continuous passage through zero, as it was the case for $\phi_{qd}=\phi_0/2$. The fact that a longitudinally asymmetric structure cannot bind the electron and have a true bound state in the fundamental propagating mode, is in agreement with Ref. 21, where a similar conclusion was derived for the straight waveguide with asymmetric dot. On further decrease of the angle ϕ_{qd} it is possible to have a reverse jump from the negative to positive Δ. For example, in Fig. 11 for $\phi_{qd}=0$ the zero of the resonance again is achieved at the smaller energies than the corresponding maximum. Switch from ''maximum-minimum'' to ''minimum-maximum'' configuration takes place at $\phi_{qd}\simeq23°$.

IV. CONCLUDING REMARKS

We have discovered a rich structure of Fano resonances in the theoretical description of the transport properties of the

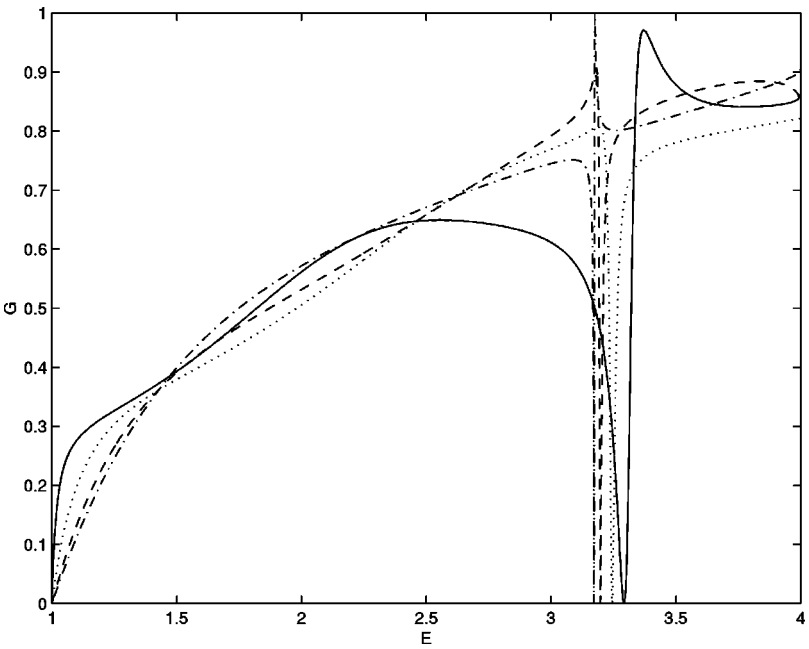

FIG. 11. Conductance G as a function of the Fermi energy for $L=0.5$, $S=0.1$, $\Omega=-4$, $\rho_0=0.01$, $\phi_0=180°$ and several values of ϕ_{qd}: the solid line is for $\phi_{qd}=0$, the dotted line is for $\phi_{qd}=30°$, the dashed line is for $\phi_{qd}=60°$, and the dash-dotted line is for $\phi_{qd}=90°$. Similar to Fig. 7, for all curves minimum conductance is an exact zero. The difference Δ is positive for $\phi_{qd}=0°$ and 90°, and negative for other two curves.

bent Q1D waveguides with embedded quantum dot. Manipulation of these resonances by the variation of the bend and dot parameters leads to a number of interesting effects which may be used in the design of nanodevices. Among these features we mention the collapse of the Fano resonances with the formation of true bound states in the continuum, and the inversion of the mutual location of the extrema of the resonance.

We considered the impurity extremely localized in the propagation direction. Generalization to the finite-range scatterer without any difficulties may be performed directly in the same way as it is done for the straight waveguide,[14,20,21] when multiple Fano resonances might appear and interact with each other.

We disregarded any atomic structure of the crystal of the waveguide. Its inclusion can modify results presented here. However, the above described phenomena should survive qualitatively in more sophisticated calculations taking into account the form of the Bloch wave functions. Also, they should serve as a basis for the treatment of the electron-electron interaction in this system when some kind of Hartree-Fock or Thomas-Fermi potential should be implemented. It is believed that for low currents in quantum waveguides Coulomb scattering does not change significantly the calculations of the independent electron theory.[56]

Experimentally, Fano resonances were observed in a number of nanostructures, such as semiconductor superlattices[10] or single-electron transistor.[62] Clean double-bend quantum wires were also fabricated, and their transport properties were studied experimentally.[63] However, interpretation of the results of these experiments is controversial with different explanation of observed peaks in the conductance.[63,64] On the one hand, improving spatial homogeneity of the curved quantum wires may help to avoid this ambiguity. On the other hand, deliberate introduction into the bend of the localized impurity should be detectable, as we have shown in this paper, as an appearance of the new dips and peaks in the conductance. Another method of observing phenomena predicted here, is the use of the electric field of the transverse-electric mode of the radio waveguide. One-to-one correspondence between electron motion in the quantum Q1D wire and electromagnetic wave propagation down the metallic waveguide is well known and was used for the experimental detection of the bound states in clean single[30] and double[65] bends.

Finally, we mention that the results presented in this paper are straightforwardly applied to the analysis not only of the electromagnetic,[36–38] but of the acoustic[43,44,66,67] waves propagation as well. First experiments on the sound passage through the defect-free bent acoustic ducts are dated as far back as mid 1970's.[40,42] Different type of the boundary conditions for the acoustic waves may lead to the shift of the wavenumbers ν_n, as it was shown in Ref. 36 for the electromagnetic waves. However, general features outlined above should not be altered. In fact, experiments have revealed that an insertion into the bend of the longitudinal rigid hard-wall vane or attenuator with impenetrable boundaries significantly alters transmission properties of the curved acoustic ducts producing new resonances with both the Breit-Wigner form or with the line shape closely reminescent that of the Fano profile.[41,42] Very recently it was proved theoretically[32] that a bent planar wire with Dirichlet and Neumann boundary conditions on the opposite sides of the waveguide possesses, under some requirements, a bound state. Accordingly, we believe that a bent acoustic duct with an appropriate soft impurity should exhibit Fano resonances too, say, on the dependence of the total transmitted sound intensity versus frequency, and their evolution should follow the one described in Sec. III.

[1] U. Fano, Phys. Rev. **124**, 1866 (1961).
[2] A. Bohm, *Quantum Mechanics* (Springer, New York, 1993), Chap. 18.
[3] H. Beutler, Z. Phys. **93**, 177 (1935).
[4] U. Fano, Nuovo Cimento **12**, 154 (1935).
[5] R.K. Adair, C.K. Bockelman, and R.E. Peterson, Phys. Rev. **76**, 308 (1949).
[6] T.K. Fang and T.N. Chang, Phys. Rev. A **57**, 4407 (1998).
[7] P. Durand, I. Paidarová, and F.X. Gadéa, J. Phys. B **34**, 1953 (2001); P. Durand and I. Paidarová, *ibid.* **35**, 469 (2002).
[8] S. Glutsch, Phys. Rev. B **66**, 075310 (2002).
[9] W. Ihra, Phys. Rev. A **66**, 020701 (2002).
[10] C.P. Holfeld, F. Löser, M. Sudzius, K. Leo, D.M. Whittaker, and K. Köhler, Phys. Rev. Lett. **81**, 874 (1998); T.W. Canzler, C.P. Holfeld, V.G. Lyssenko, D.M. Whittaker, K. Köhler, and K. Leo, Phys. Status Solidi A **178**, 39 (2000).
[11] E.R. Racec and U. Wulf, Phys. Rev. B **64**, 115318 (2001).
[12] J.U. Nöckel and A.D. Stone, Phys. Rev. B **51**, 17 219 (1995).
[13] C.S. Chu and R.S. Sorbello, Phys. Rev. B **40**, 5941 (1989).
[14] P.F. Bagwell, Phys. Rev. B **41**, 10 354 (1990); J. Phys.: Condens. Matter **2**, 6179 (1990).
[15] E. Tekman and S. Ciraci, Phys. Rev. B **42**, 9098 (1990).
[16] J.U. Nöckel, Phys. Rev. B **46**, 15 348 (1992).
[17] E. Tekman and P.F. Bagwell, Phys. Rev. B **48**, 2553 (1993).
[18] J.U. Nöckel and A.D. Stone, Phys. Rev. B **50**, 17 415 (1994).
[19] C.S. Kim and A.M. Satanin, Zh. Éksp. Teor. Fiz. **115**, 211 (1999) [JETP **88**, 118 (1999)].
[20] C.S. Kim, A.M. Satanin, Y.S. Joe, and R.M. Cosby, Phys. Rev. B **60**, 10 962 (1999); Zh. Éksp. Teor. Fiz. **116**, 263 (1999) [JETP **89**, 144 (1999)].
[21] C.S. Kim, O.N. Roznova, A.M. Satanin, and V.B. Stenberg, Zh. Éksp. Teor. Fiz. **121**, 1157 (2002) [JETP **94**, 992 (2002)].
[22] B.J. van Wees, H. van Houten, C.W.J. Beenakker, J.G. Williamson, L.P. Kouwenhoven, D. van der Marel, and C.T. Foxon, Phys. Rev. Lett. **60**, 848 (1988).
[23] D.A. Wharam, T.J. Thornton, R. Newbury, M. Pepper, H. Ahmed, J.E.F. Frost, D.G. Hasko, D.C. Peacock, D.A. Ritchie, and G.A.C. Jones, J. Phys. C **21**, L209 (1988).
[24] P. Duclos and P. Exner, Rev. Math. Phys. **7**, 73 (1995).
[25] J. T. Londergan, J. P. Carini, and D. P. Murdock, *Binding and Scattering in Two-Dimensional Systems: Applications to Quantum Wires, Waveguides, and Photonic Crystals* (Springer-Verlag, Berlin, 1999).
[26] R.L. Schult, D.G. Ravenhall, and H.W. Wyld, Phys. Rev. B **39**, 5476 (1989).
[27] P. Exner, Phys. Lett. A **141**, 213 (1989); P. Exner and P. Šeba, J. Math. Phys. **30**, 2574 (1989); P. Exner, P. Šeba, and P. Štoviček, Chech. J. Phys. B **39**, 1181 (1989); Phys. Lett. A **150**, 179 (1990); M.S. Ashbough and P. Exner, *ibid.* **150**, 183 (1990); P. Exner, J. Phys. A **28**, 5323 (1995); P. Duclos, P. Exner, and D. Krejčiřík, Ukr. Fiz. Zh. **45**, 595 (2000) [Ukr. Phys. J. **45**, 595 (2000)]; Commun. Math. Phys. **223**, 13 (2001); P. Exner and T. Ichinose, J. Phys. A **34**, 1439 (2001); P. Exner and D. Krejčiřík, *ibid.* **34**, 5969 (2001).
[28] D.W.L. Sprung, H. Wu, and J. Martorell, J. Appl. Phys. **71**, 515 (1992).
[29] J. Goldstone and R.L. Jaffe, Phys. Rev. B **45**, 14 100 (1992).
[30] J.P. Carini, J.T. Londergan, K. Mullen, and D.P. Murdock, Phys. Rev. B **46**, 15 538 (1992); **48**, 4503 (1993).
[31] K. Lin and R.L. Jaffe, Phys. Rev. B **54**, 5750 (1996).
[32] J. Dittrich and J. Kříž, J. Phys. A **35**, L269 (2002).
[33] F. Sols and M. Macucci, Phys. Rev. B **41**, 11 887 (1990).
[34] K. Vacek, H. Kasai, and A. Okiji, J. Phys. Soc. Jpn. **61**, 27 (1992); K. Vacek, A. Okiji, and H. Kasai, Phys. Rev. B **47**, 3695 (1993).
[35] O. Olendski and L. Mikhailovska, Phys. Rev. B **66**, 035331 (2002).
[36] J.A. Cochran and R.G. Pecina, Radio Sci. **1**, 679 (1966).
[37] L. Lewin, D. C. Chang, and E. F. Kuester, *Electromagnetic Waves and Curved Structures* (Peter Peregrinus, Stevenage, UK, 1977).
[38] B. Z. Katsenelenbaum, L. Mercader del Río, M. Pereyaslavets, M. Sorolla Ayza, and M. Thumm, *Theory of Nonuniform Waveguides* (IEE, London, UK, 1998).
[39] F.E. Grigor'yan, Akust. Zh. **14**, 376 (1968) [Sov. Phys. Acoust. **14**, 315 (1969)]; W. Rostafinski, J. Acoust. Soc. Am. **52**, 1411 (1972); **56**, 11 (1974); **56**, 1005 (1974); **60**, 23 (1976).
[40] A. Cummings, J. Sound Vib. **35**, 451 (1974); W.C. Osborne, *ibid.* **45**, 39 (1976).
[41] C.R. Fuller and D.A. Bies, J. Acoust. Soc. Am. **63**, 681 (1978); J. Sound Vib. **56**, 45 (1978).
[42] A. Cabelli, J. Sound Vib. **68**, 369 (1980).
[43] S. Félix and V. Pagneux, J. Acoust. Soc. Am. **110**, 1329 (2001).
[44] W. Rostafinski, *Monograph on Propagation of Sound Waves in Curved Ducts* (NASA Scientific and Technical Information Division, Washigton, D.C., 1991).
[45] F. Lenz, J.T. Londergan, E.J. Moniz, R. Rosenfelder, M. Stingl, and K. Yazaki, Ann. Phys. (N.Y.) **170**, 65 (1986).
[46] H. Eyring, J. E. Walter, and G. E. Kimball, *Quantum Chemistry* (Wiley, New York, 1944), Chap. 16.
[47] K.T. Tang, B. Kleinman, and M. Karplus, J. Chem. Phys. **50**, 1119 (1969).
[48] *Handbook of Mathematical Functions*, edited by M. Abramowitz and I. A. Stegun (Dover, New York, 1964).
[49] S. Flügge, *Practical Quantum Mechanics* (Springer, Berlin, 1971), Vol. 1.
[50] O. Olendski and C.S. Kim, J. Phys.: Condens. Matter **8**, 2197 (1996).
[51] R. Landauer, IBM J. Rev. Dev. **1**, 223 (1957); Philos. Mag. **21**, 863 (1970).
[52] J. von Neumann and E. Wigner, Z. Phys. **30**, 465 (1929).
[53] F.H. Stillinger and D.R. Herrick, Phys. Rev. A **11**, 446 (1975); H. Friedrich and D. Wintgen, *ibid.* **31**, 3964 (1985); **32**, 3231 (1985).
[54] E.N. Bulgakov, P. Exner, K.N. Pichugin, and A.F. Sadreev, Phys. Rev. B **66**, 155109 (2002).
[55] L. D. Landau and E. M. Lifshitz, *Quantum Mechanics (Non-Relativistic Theory)* (Pergamon, New York, 1977).
[56] C.S. Lent, Appl. Phys. Lett. **57**, 1678 (1990).
[57] S. Chaudhuri, S. Bandyopadhyay, and M. Cahay, Phys. Rev. B **45**, 11 126 (1992); Z.-L. Ji and K.-F. Berggren, *ibid.* **45**, 6652 (1992).
[58] K.-F. Berggren and Z.-L. Ji, Phys. Rev. B **47**, 6390 (1993).
[59] J. Goldstein, C. Lebiedzik, and R.W. Robinett, Am. J. Phys. **62**, 612 (1994).
[60] O. Olendski, J. Phys.: Condens. Matter **7**, 5067 (1995).
[61] M. Born and E. Wolf, *Principles of Optics* (Cambridge University Press, Cambridge, 1999).
[62] J. Göres, D. Goldhaber-Gordon, S. Heemeyer, M.A. Kastner, H.

Shtrikman, D. Mahalu, and U. Meirav, Phys. Rev. B **62**, 2188 (2000).
[63] J.C. Wu, M.N. Wybourne, W. Yindeepol, A. Weisshaar, and S.M. Goodnick, Appl. Phys. Lett. **59**, 102 (1991).
[64] J.P. Carini, J.T. Londergan, and D.P. Murdock, Phys. Rev. B **55**, 9852 (1997).
[65] J.P. Carini, J.T. Londergan, D.P. Murdock, D. Trinkle, and C.S. Yung, Phys. Rev. B **55**, 9842 (1997).
[66] P. M. Morse and K. U. Ingard, *Theoretical Acoustics* (Princeton University Press, Princeton, 1986), Chap. 9.
[67] D. T. Blackstock, *Fundamentals of Physical Acoustics* (Wiley-InterScience, New York, 2000), Chap. 6.